2023 IEEE International Conference on Robotics and Automation (ICRA 2023)
May 29 - June 2, 2023. London, UK

Towards Multi–Day Field Deployment Autonomy: A Long–Term Self–Sustainable Micro Aerial Vehicle Robot

Stephen J. Carlson, Prateek Arora, Tolga Karakurt, Brandon Moore, Christos Papachristos

***Abstract*— This works deals with the problem of long-term autonomy in the context of multi-day field deployments of Micro Aerial Vehicle (MAV) systems. To truly depart from the necessity for human intervention for the crucial task of providing battery recharging, and to liberate from the need to operate in a confined range around specially installed infrastructure such as recharging pods, the MAV robot is required to harvest power on its own, but equally importantly also sustain prolonged periods of ambient power scarcity. This implies being able to sustain the battery charge overnight when using solar recharging, or even during multiple days of illumination inadequacy (e.g., due to degraded atmospheric lucidity and heavy overcast). We address this by presenting a Self-Sustainable Autonomous System architecture for MAVs centered around a specially tailored Power Management Stack, which is capable of achieving deep system hibernation, a feature that facilitates the aforementioned functionalities. We present a) continuous, b) multi-day successive, and c) externally-powered recharging that uses a legged robot-mounted Mobile Recharging Station. We conclude by demonstrating a challenging zero-intervention multi-day field deployment mission in the N.Nevada region.**

I. INTRODUCTION

Autonomy has monopolized the world of robotics research over recent years, generating a cataclysmic sequence of technological advances enabling the unsupervised simultaneous exploration and mapping of unknown GPS-denied environments [1–11], the systematic 3D reconstruction and inspection of known infrastructure assets [12–14], the rapid deployment of remote sensing swarms to aid in perceptually-challenging emergency response situations [15–18], as well as planetary exploration missions [19]. Moreover, the miniaturization of the corresponding robotic (sub)systems is quickly advancing, yielding increasingly versatile and attritable solutions whose rapid fabrication and mass deployment presents unprecedented opportunities.

A key requirement for *long-term* autonomy however, is for the robot to be capable of sustaining its operation over prolonged periods of time without requiring human attention. At the most fundamental level, this refers to the robot recharging its battery on its own. Commercially successful examples range from early household service robotics with dedicated charging stations [20], to more recent industrial service robots [21, 22] as well as drones [23–25] that follow the same "localize and return home to recharge" approach, all being indicative of the prominence of a new generation of hands-off robotic solutions.

Fig. 1: Indicative instances of the hybrid micro aerial Self-Sustained Autonomous System (SSAS), capable of solar – and externally supplied– power harvesting, as well as hyper-efficient recharging relying on full systems hibernation.

For field robotics deployed into the wild and/or unstructured environments to unlock this capacity, a self-sufficient recharging architecture is required that allows to harvest ambient power when available, but equally importantly to sustain their stored energy and maintain their battery in a good state during a prolonged period of input power scarcity. For the case of Micro Aerial Vehicles (MAVs), the design of such a system presents additional challenges so as to remain compatible with their miniaturized form.

This work contributes a complete Power Management architecture for such a system tailored around an autonomous micro tiltrotor hybrid aerial robot, capable of performing a) solar recharging in overcast, hazy-atmosphere, shaded, and generally non-ideal field conditions, but also b) hibernation of all power-draining subsystems during the absence of sunlight –e.g. overnight– to conserve its battery, with periodic low-power wakeup operation to reassess the situation. As an addition, the same architecture also integrates a versatile c) external power recharging option, to fast-recharge from docking with static or even mobile charging stations carried by ground-based autonomous agents. Overall, with these contributions we develop a novel class of a micro aerial Self-Sustained Autonomous System (SSAS) shown in Figure 1, which is fielded in a real multi-day mission conducted in N.Nevada, in challenging atmospheric lucidity conditions due to a heavy smoke plume from a local megafire.

In the remainder of the paper, Section II presents related work, Section III details the system design aspects, Section IV presents its distinct modes of operation, and Section V demonstrates unsupervised multi-day field testing results.

This material is based upon work supported by the NASA Award: *ULI: Robust and Resilient Autonomy for Advanced Air Mobility* and the NSF Award: *2008904: RI: Small: Learning Resilient Autonomous Flight*. The presented content and ideas are solely those of the authors.

The authors are with the University of Nevada, Reno, 1664 N. Virginia, 89557, Reno, NV, USA stephen_carlson@nevada.unr.edu

2023 IEEE International Conference on Robotics and Automation (ICRA) | 979-8-3503-2365-8/23/$31.00 ©2023 IEEE | DOI: 10.1109/ICRA48891.2023.10161014

II. RELATED WORK

Aerial robotic recharging approaches [26–42] have been widely explored by the robotics community, aiming to extend their flight time to facilitate persistent operation and to minimize the reliance on humans to replenish their battery. Many approaches [26–30] rely on stationary charging stations, where the UAVs dock to recharge, while other recent works [31, 32] address recharging via contactless wireless power transmission. Some works propose to leverage mobile ground robots either by having the aerial robot dock onto them [33] or by utilizing manipulation [34] to grasp the UAV and subsequently swap out the batteries. Such systems remain constrained to a bounded span of operation along with incurring higher cost due to their reliance on additional robotic systems or charging infrastructure. Moving to the domain of self-sustainable approaches, the authors of AtlantikSolar [35, 43, 44] and SAUV [36] designed fixed–wing aerial vehicles optimized for continuous flight, persisting beyond the 24hr mark by utilizing solar arrays installed on their wings and integrating on-board solar harvesting modules. Despite the impressive feat of extended continuous flight, due to their super-lightweight optimization these vehicles cannot takeoff autonomously once landed, requiring hand launch to perform back-to-back missions. The Airbus® Zephyr™ fixed-wing solar aircraft [45] has a wingspan of 25m to achieve continuous flight for over months at a time, however its scale does not translate to micro aerial robotics applications, and restricts its application to above-weather and conventional air traffic. More recent works [37, 38] present a 2.15m wingspan transformable solar-UAV, with the ability to switch between the fixed–wing and Vertical Take-Off and Landing (VTOL) configurations. This allows to resume solar harvesting while landed, but this specific design has a suboptimal configuration of solar array w.r.t. the sun. The authors of [46, 47] overcome this while also focusing on a multi-hop mission profile (though in aquatic settings). Neither of these can however qualify as a long-term SSAS, as they lack the fundamental capacity to tackle prolonged periods of inadequate ambient power input (and manage their battery) in their duration, which is a realistic requirement considering their intended *fully autonomous multi-day* operational profile.

To this end, we propose an overall SSAS architecture that is applicable for a versatile hybrid VTOL / fixed-wing micro aerial robot which also integrates high-level autonomy capabilities and a solar panel wing design. Our key contribution that unlocks the capacity for true *autonomous multi-day* operation is the accommodation of deep hibernation capabilities at under 5mW, which allows the vehicle to remain in weeks-long stasis during periods of ambient power scarcity, or simply retain its battery capacity overnight super-efficiently. We accompany this contribution with an open-source design that respects the operational and miniaturization / low-weight constraints, allowing to maintain the rapid-reproducibility to unlock cost-effective swarming multi-day deployments. Finally, we contribute an extension for fast-recharging with mobile docking stations mounted on legged field robots.

III. SYSTEM DESIGN

This section elaborates the design and implementation aspects of the proposed system architecture enabling self-sustained multi-day deployments of an autonomous MAV.

A. System Overview

The core components of the reconfigurable micro aerial Self-Sustained Autonomous System (SSAS) are illustrated in Figure 2, together with the specific hardware design.

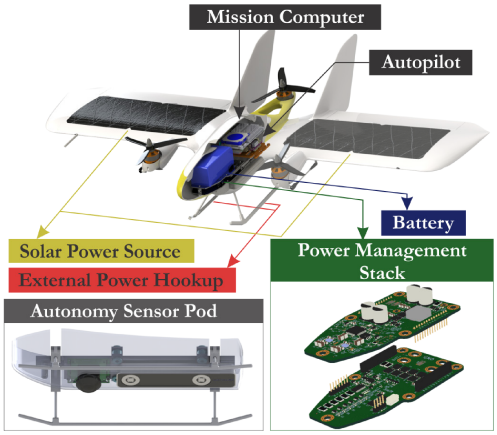

Fig. 2: Overview of the architecture of the reconfigurable micro aerial Self-Sustained Autonomous System (SSAS). Detail: Vibration-isolated Autonomy Sensor Pod and landing skids hosting External Power Hookups. Power Management Stack of in-house designed Printed Circuit Boards (PCBs).

The Mission Computer and the Autonomy Sensor Pod –which comprises a custom-designed vibration-isolating mount with a downwards-facing Visual-Inertial tracking & mapping sensor (Intel® RealSense™ T265) and a 1080p 30Hz RGB camera with a 180^o Field-of-View lens– are responsible for all high-level perception operations and path/mission planning operations. The Autopilot (mRo® PixRacer™ Pro) handles the hovering, fixed-wing, and transition flight control of the hybrid aircraft, based on waypoints forwarded to it by the Mission Computer.

The Power Management Stack is the critical component which unlocks the ability to perform self-sustained multi-day deployments by monitoring and recharging the battery, using solar power harvesting, while at the same time offering the versatility to fast-charge from external power sources that may be available in the field. For the latter case, the vehicle's landing skids mechanism can accommodate conductive wires routed to the Power Management Stack and lend themselves as External Power Hookups, while for the primary self-sustained recharging case, an array of SunPower® MAXEON™ solar cells which form the wing airfoil upper surfaces is used.

The rapid prototyping-based design is open-access https://github.com/StephenCarlson/MiniHawk-VTOL.

B. Recharging & Hibernation Power Management

The Power Management Stack block diagram shown and discussed in Figure 3 comprises a DC–DC Converter, Battery Management System (BMS), Load Switch, I/O Interfaces, and other features as shown, to support self-sustained operations and hibernation in the field. The DC–DC Converter uses a combined Buck-Boost Topology with N-Channel MOSFETs stimulated by Charge Pump drivers, and can measure the voltage and current on the stage inputs and outputs. The Load Switch comprises a parallel cascade of MOSFETs in the double-switch configuration to prevent backdriving from the system load. The BMS measures the battery cell voltage and current, and balances individual cells using a switched power resistor array. Self-calibration and thermal sensing are also included in this subsystem. The entire device is managed by an ARM® Cortex-M4F 32-bit Micro-Controller Unit (MCU) with isolated serial interfaces for connecting to a managing autopilot or single-board computer. The system also accommodates datalogging to an onboard SPI Flash device, and in addition to the aircraft main bus can switch an auxiliary load (a resistive heater) for cold-weather operations.

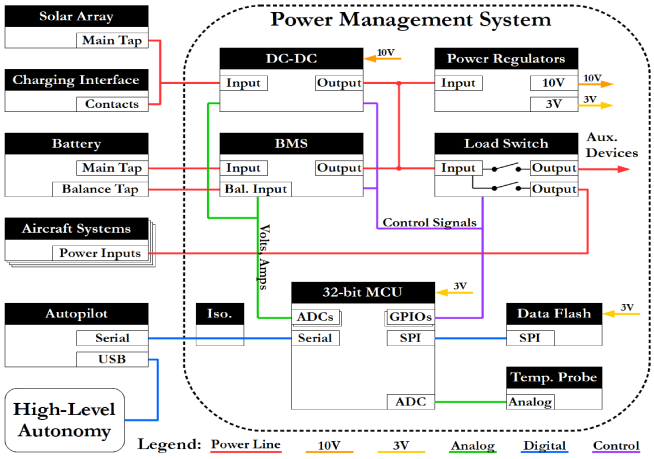

Fig. 3: Overview of the Power Management Stack. Power Input from either the wing-mounted solar array or the charging contacts on the landing legs feed the DC–DC converter. The battery connects to the Battery Management Subsystem for precision cell voltage monitoring and maintenance. All aircraft power is switched by the Power Management System, allowing for deep power conservation. The Power Management System is controlled by the aircraft autopilot through a digitally-isolated serial connection. All High–Level Autonomy actions are communicated to the autopilot through a USB connection from the High–Level compute element.

Particularly important system design features are:

i) Very-low-power consumption in regular operation and when in hibernation. The power consumed by the system during energy harvesting is around 300mW, and less than 5mW when powered down in hibernation.

ii) A failsafe load switch trigger that is reinforced against spurious deactivation of the aircraft power bus in instances where the managing MCU is damaged or malfunctioning. It guarantees that the aircraft always remains powered, except only when two distinct lines are driven at specific voltage levels by the host MCU (a combined state which can only occur when hibernation is actually intended).

The Power Management Stack opportunistically charges the aircraft battery whenever the input presents a sufficient electrical source. The system can efficiently charge the battery at rates as high as 25W and as low as 350mW, drawing from either the solar array or an external charging pad while isolating both pathways using OR-ing power diodes. As shown and discussed in the State Machine Figure 4, the battery is charged in a Constant-Current, Constant-Voltage sequence until charge current diminishes to zero, at which point the battery is considered charged and the system can wake the aircraft from hibernation. If power is interrupted during charging while the aircraft is hibernated, the Power Management Stack will sleep while periodically sampling the input to resume charging when the source (either sunlight or charging pad) returns. If the source exhibits an I–V curve, such as a solar array, then during charging the system finds the Maximum Power Point, compensating for variations induced by changes in temperature and illumination.

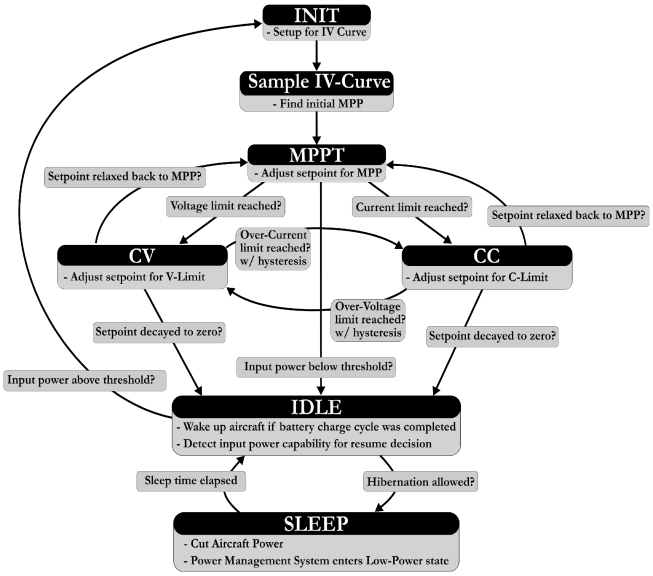

Fig. 4: Power Management Stack states. Whenever possible, the device will opportunistically charge the battery whether the aircraft is powered or hibernated. If the battery reaches full charge, the aircraft is powered on. If hibernation has been requested by the aircraft autonomy stack, the Power Management Stack cuts aircraft power until the battery is charged or until a specified time has elapsed. Constant–Current and Constant–Voltage states are entered where current or voltage limits are reached, respectively, and alter the DC–DC Converter setpoint behavior to remain within these limits. The MPPT state perturbs the DC–DC converter setpoint to identify the peak power region of the solar array.

The autopilot stack handles communication with the Power Management Stack through a UART serial link. To enforce a tight coupling between actual aircraft flight state and safe activation of hibernation, the final authority for issuing a hibernation command to the Power Management

Stack is retained by the Autopilot. The Mission Computer interface can indicate to the Autopilot stack *readiness* to launch or to hibernate, which allows for the High-Level stack to compose waypoint missions and upload them prior to launch, or to finalize pending Operating System kernel tasks before the aircraft power is cut by hibernation.

C. High–Level Autonomy

The autonomy capabilities of the SSAS are supported by Khadas® VIM3™, a powerful small-sized companion computer supporting the Robot Operating System (ROS), and with a built-in Neural Processing Unit (NPU) that allows us to perform efficient forward inference of neural networks. This is interfaced with the Autonomy Sensor Pod as well as the Autopilot, and is responsible for managing normal mission planning & waypoints, as well as to autonomously detect candidate landing sites using aerial imagery (e.g. for GPS-degraded /emergency landing per prior work [48], and for Mobile Charging Station recharging as we demonstrate followingly). The extremely lightweight YOLOX-Nano [49] deep neural network with 0.91M parameters which follows an anchor–free architecture is tailored towards this use.

IV. SYSTEM OPERATION

This section details the operational modes of the Power Management Stack with corresponding experimental data.

A. Continuous Solar Recharging

This refers to a standard solar recharging cycle where the ambient power consistently remains above the minimum input power threshold value of $P_{in}^{min} = 350$mW. The system design facilitates harvesting energy at such a low threshold, which allows to recharge uninterruptedly during a nominal overcast day with periods of cloud coverage. Such a sequence is illustrated in Figure 5, initiating at the early morning hours with a 1300mAh battery in a non-deeply-discharged state, and completing the charge around the 4hr mark. The input power is shown with a yellow line, and the power flowing into the battery with a dashed orange line, indicating the power efficiency of our design around these nominal operating conditions. The power fluctuation is indicative of the common-case overcast conditions that this sequence was captured in. The blue line illustrates the voltage rise of the battery as it's being recharged, and the green line corresponds to the estimated recharged capacity since the beginning of the sequence. Lastly, we also present the Boost converter duty cycle setpoint control with a magenta line.

It is highlighted that this is considered as a nominal operational case; Figure 6 additionally illustrates the system's capabilities at both a more challenging, as well as a more favorable set of operating conditions: The left subfigure shows the effect of direct shading due to a nearby structure's shadow rolling over the vehicle during the afternoon hours (around the 2pm timepoint). Despite this unfavorable recharging site selection, the recharging operation proceeds since the P_{in}^{min} is not violated. The right subfigure shows the result reported in [50] with an early iteration of a solar recharge-capable system, where sunlight was direct and consistent during almost the entire sequence.

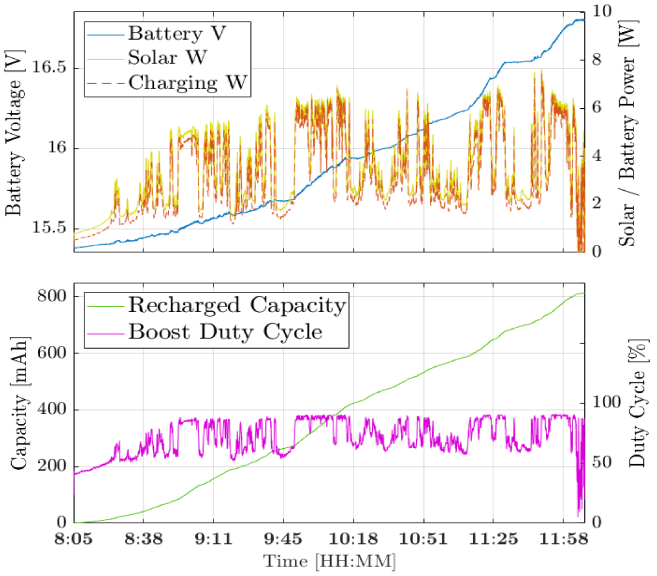

Fig. 5: Solar-powered continuous charging sequence captured during the morning hours of an overcast day.

This favorable situation is indicative by the consistent operation around $P_{in} = 6$W, which was the maximum expected during that time of year, and the outcome of recharging a deeply-depleted battery in $\simeq 4$hrs.

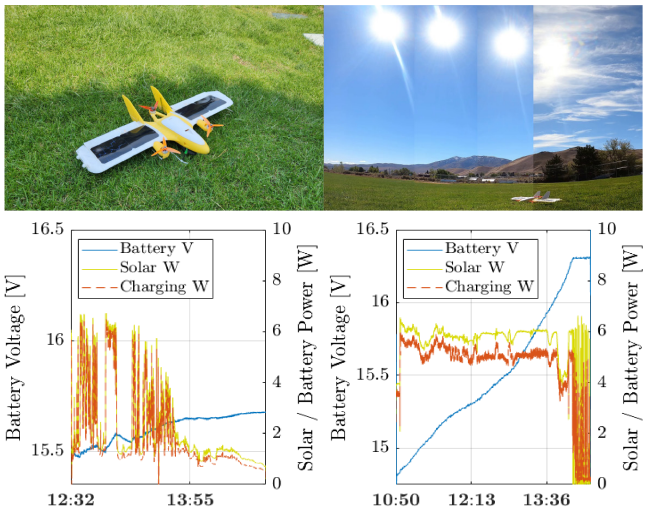

Fig. 6: Indicative solar-recharging sequence demonstrating worst-and-best case operating points.

B. Multi-Day Successive Recharging

The most important contribution of our proposed design that unlocks multi-day field deployment capabilities for micro aerial robotics, is the capacity for full-system hibernation, which conserves the battery capacity overnight and during prolonged periods of ambient power scarcity. Figure 7 illustrates this, whereby the overnight hibernation period is illustrated with the grey-shaded area. It is highlighted that recharging inhibits all major power outflows, but hibernation additionally brings the managing MCU in low-power mode with all unnecessary peripherals disabled, other

than a periodic 10min wakeup. Specifically for the case of the experimental data presented in this Section, we additionally enabled datalogging capabilities.

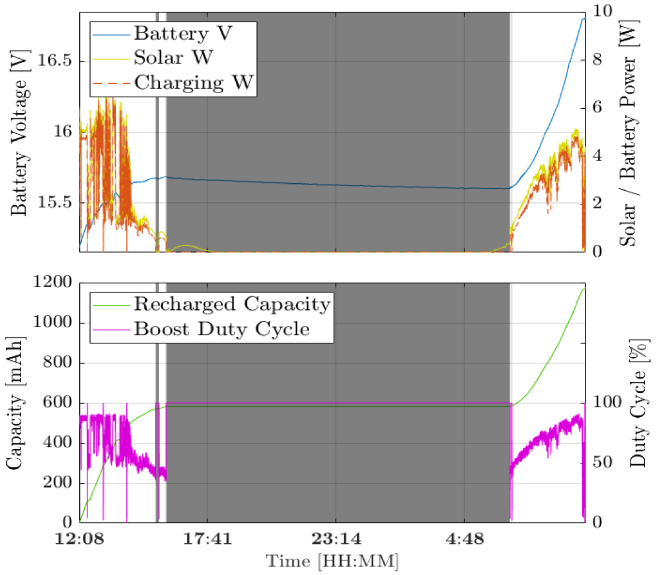

Fig. 7: Multi-day solar-powered recharging sequence with overnight hibernation.

It can be observed that around the 3:30pm time mark the system initiates a first hibernation period due to the low ambient power; we speculate this to be triggered by a combination of a low sun angle together with temporary cloud coverage. The system subsequently exits hibernation once the P_{in}^{min} is surpassed, but eventually re-enters around the 4pm mark. Datalogging in wakeup instances allows us to observe the dying down of the input solar power (yellow line) until the 6:30am time mark where it starts rising again. The charge power flow to the battery (dashed orange line) is zero and the recharged capacity constant since no charging takes place. The battery voltage slowly drops by $\simeq$ 0.1V overnight, as is common with the resting voltage for Li-Po batteries. Eventually the system exits hibernation and recharges to its full capacity. It is noted that this recharging sequence was particularly challenging, as it was conducted under heavy fire plume conditions of a nearby megafire impacting atmospheric lucidity.

C. Externally Powered Recharging

An additional contribution of our proposed system is the capacity to leverage external sources to harvest power. On one hand, this is a functionality and design specification of the Power Management Stack, which is capable of handling the high-power recharging. On the other hand, the SSAS design is configured such that the landing skids are able to house conductive wires to facilitate external charging. The port side skid is lined with a cable that is routed to the positive side of the Power Management Stack, while the starboard side hosts the negative connection. Wire routing runs along the vertical skid support into the vehicle allowing current flow into the Power Management Stack, which tests for if the input can develop more than 500mA consistently when drawn, to decide whether to initiate the externally-powered recharging. An input voltage of 25V can be safely handled on the input side, and a typical safe input power while charging is the range of $\simeq$ 25-30W. This feature is developed in order to facilitate fast-recharging in the field, either by leveraging dedicated charging stations, but more interestingly also mobile ones, carried by ground robots that may be deployed as part of a heterogeneous robot swarm in the context of the same long-term field mission. Specifically towards this vision, we developed a Mobile Charging Station (MCS) which is tailored for the Boston Dynamics® Spot™ legged robot. This is illustrated in Figure 8.

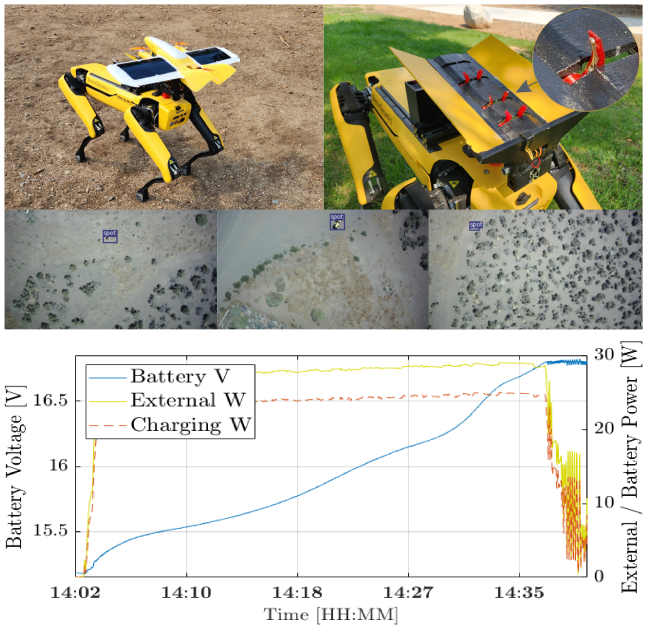

Fig. 8: Externally-powered recharging sequence and MCS.

In the top row, the SSAS configuration when landed onto the Mobile Docking Station is seen, as well as the proposed design. The SSAS is secured into place using retaining structures to grasp the skids. Two of these active claw-like mechanisms are integrated into the design, one port side and one starboard side; these revolve to snap the SSAS skids into place. On one hand, this feature allows for the Spot™ robot to continue its dynamic walking as it proceeds with its own mission, in a marsupial multi-system approach [51]. On the other hand, the center claws on either side are laced with conductive material –shown detail callout on the figure– that comes into contact with the skid-embedded wires. The claw material is compliant and the mechanism holds the skids in tension, such that the electrical connection remains uninterrupted. The bottom row demonstrates such an externally-powered recharging cycle. As expected, the gained advantage is the ability to fully recharge in a little over 30min, which can be leveraged in the context of long-term deployments to perform quick mission jumps between MCSs moving throughout a wide area. We also demonstrate in the middle row the ability to leverage the SSAS High-Level Autonomy to detect the precise relative location of an MCS using our Deep-Learned network, re-trained on

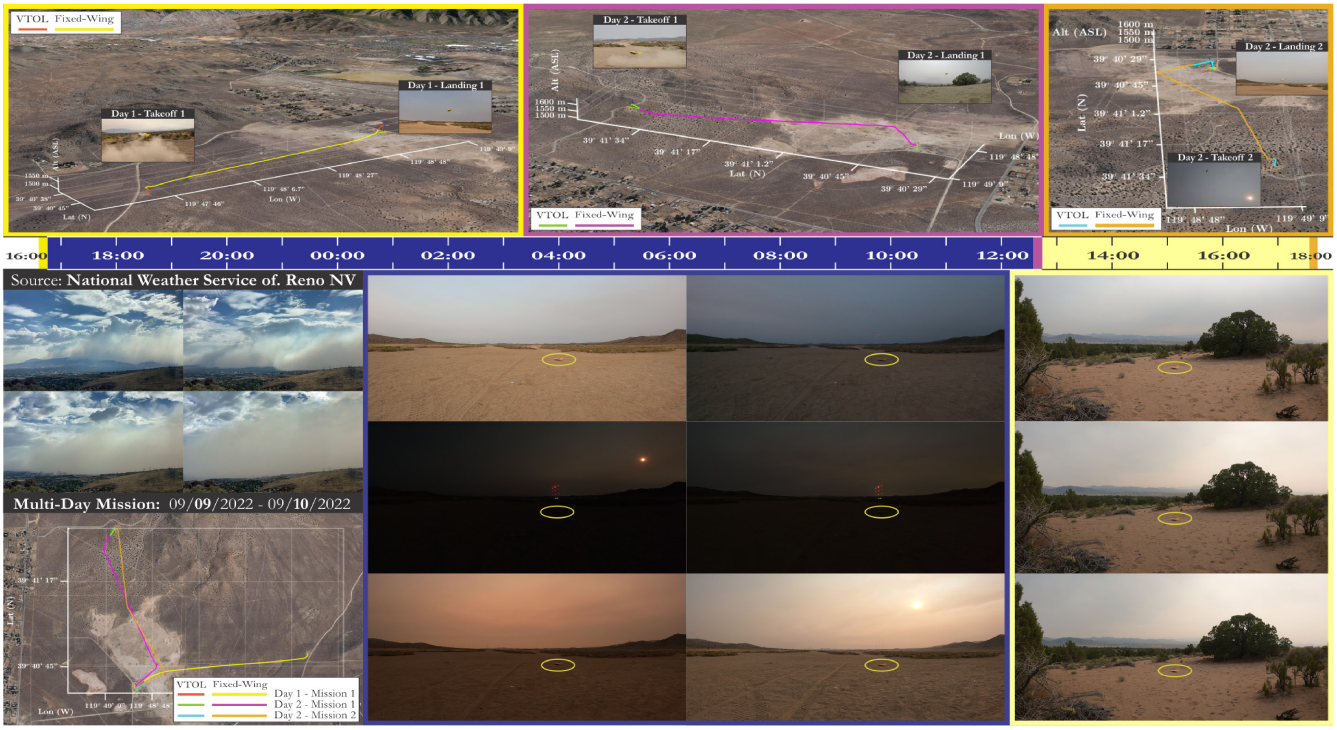

Fig. 9: Multi-day (9-10 Sept. 2022) field testing with the SSAS. Top: Distinct 3 mission legs. Below: Timeline with color-coded sections for flight and recharging sequences. Bottom: Mission / environment overview, and recharging timelapses.

aerial visual imagery of the Spot™ robot (with the custom MCS backpack) in relevant unstructured environments of N.Nevada. This is an extension of the terrain landmark detection & classification framework for emergency vision-based landing, as demonstrated in prior own work [48].

V. EXPERIMENTAL STUDY

We experimentally validated the SSAS in a multi-day field deployment mission in N.Nevada, with the corresponding results illustrated in Figure 9. More specifically, three mission legs were executed overall in an approximate duration of 24hrs. The top row shows them all georeferenced and in time order, each within a differently-colored box outline, namely [Gold]: Day 1 - Mission 1, [Magenta]: Day 2 - Mission 1, [Orange]: Day 2 - Mission 2. The timepoint of execution for each corresponding leg is placed color-coded on the Timeline bar, shown in the row below them.

Below the Timeline bar, the center and rightmost columns correspond to timelapses of the recharging cycles between successive missions, again with each being within a separately-colored box outline, namely [Blue (middle 2 columns)]: Overnight recharging between Day 1 - Mission 1 and Day 2 - Mission 1, [Yellow (last column)]: Morning recharging between Day 2 - Mission 1 and Day 2 - Mission 2. A callout to the SSAS while landed and recharging/hibernating is marked with a yellow ellipsoid. The overnight recharging cycle lasted from 5:45pm to 12:30pm and relied on the successful hibernation functionality contributed by this design. The Morning recharging session lasted from 12:45pm to 5:30pm.

The left column bottom subfigure shows the 3 overall legs, maintaining the same line color-coding as the first row, which also helps distinguish between the VTOL ascent and descent, and the Fixed-Wing flight segments. Although the entire multi-day sequence was executed with zero interactions from our crew, at any point the SSAS had to be within Visual Line-of-Sight to remain within FAA regulations; under these limitations, the mission was designed to account for visual range and obstructions during each mission leg, avoiding the mountain volume seen in the middle of the subfigure.

Finally, we highlight the active conditions under which this field test was executed, by showcasing weather camera footage from the Reno Office of the National Weather Service. During these days, an active fire plume from the California Mosquito megafire had descended into the valley and remained trapped therein. This heavily degraded the atmospheric lucidity, as can be seen in all timelapses and takeoff / landing callouts provided in the figure. Despite these conditions our SSAS managed to successfully perform three mission legs, requiring two intermediate charging sequences –with one overnight–, within a multi-day period of field deployment into the wild, with zero interventions.

VI. CONCLUSIONS

We presented the architecture for a micro aerial Self-Sustainable Autonomous System, with particular focus on a novel Power Management Stack. This is responsible for recharging using solar/external power, managing the battery state, and hibernating to provide efficient recharging, as well as capacity-preservation during power scarcity periods. We experimentally demonstrated the system across its operating modes, and concluded with a multi-day field test.

REFERENCES

[1] M. Tranzatto, F. Mascarich, L. Bernreiter, C. Godinho, M. Camurri, S. M. K. Khattak, T. Dang, V. Reijgwart, J. Loeje, D. Wisth, S. Zimmermann, H. Nguyen, M. Fehr, L. Solanka, R. Buchanan, M. Bjelonic, N. Khedekar, M. Valceschini, F. Jenelten, M. Dharmadhikari, T. Homberger, P. De Petris, L. Wellhausen, M. Kulkarni, T. Miki, S. Hirsch, M. Montenegro, C. Papachristos, F. Tresoldi, J. Carius, G. Valsecchi, J. Lee, K. Meyer, X. Wu, J. Nieto, A. Smith, M. Hutter, R. Siegwart, M. Mueller, M. Fallon, and K. Alexis, "Cerberus: Autonomous legged and aerial robotic exploration in the tunnel and urban circuits of the darpa subterranean challenge," *Field Robotics*, pp. 274–324, arXiv.2201.07 067, 2021.

[2] M. Kulkarni, M. Dharmadhikari, M. Tranzatto, S. Zimmermann, V. Reijgwart, P. De Petris, H. Nguyen, N. Khedekar, C. Papachristos, L. Ott *et al.*, "Autonomous teamed exploration of subterranean environments using legged and aerial robots," in *2022 International Conference on Robotics and Automation (ICRA)*. IEEE, 2022, pp. 3306–3313.

[3] M. Tranzatto, T. Miki, M. Dharmadhikari, L. Bernreiter, M. Kulkarni, F. Mascarich, O. Andersson, S. Khattak, M. Hutter, R. Siegwart *et al.*, "Cerberus in the darpa subterranean challenge," *Science Robotics*, vol. 7, no. 66, p. eabp9742, 2022.

[4] T. Dang, F. Mascarich, S. Khattak, H. Nguyen, H. Nguyen, S. Hirsh, R. Reinhart, C. Papachristos, and K. Alexis, "Autonomous search for underground mine rescue using aerial robots," in *2020 IEEE Aerospace Conference*. IEEE, 2020, pp. 1–8.

[5] T. Dang, F. Mascarich, S. Khattak, C. Papachristos, and K. Alexis, "Graph-based path planning for autonomous robotic exploration in subterranean environments," in *2019 IEEE/RSJ International Conference on Intelligent Robots and Systems (IROS)*. IEEE, 2019, pp. 3105–3112.

[6] T. Dang, F. Mascarich, S. Khattak, H. Nguyen, N. Khedekar, C. Papachristos, and K. Alexis, "Field-hardened robotic autonomy for subterranean exploration," *Field and Service Robotics (FSR)*, 2019.

[7] S. Khattak, C. Papachristos, and K. Alexis, "Keyframe-based thermal–inertial odometry," *Journal of Field Robotics*, vol. 37, no. 4, pp. 552–579, 2020.

[8] C. Papachristos, S. Khattak, F. Mascarich, T. Dang, and K. Alexis, "Autonomous aerial robotic exploration of subterranean environments relying on morphology–aware path planning," in *2019 International Conference on Unmanned Aircraft Systems (ICUAS)*. IEEE, 2019, pp. 299–305.

[9] R. Reinhart, T. Dang, E. Hand, C. Papachristos, and K. Alexis, "Learning-based path planning for autonomous exploration of subterranean environments," in *2020 IEEE International Conference on Robotics and Automation (ICRA)*. IEEE, 2020, pp. 1215–1221.

[10] C. Papachristos, S. Khattak, and K. Alexis, "Uncertainty-aware receding horizon exploration and mapping using aerial robots," in *2017 IEEE international conference on robotics and automation (ICRA)*. IEEE, 2017, pp. 4568–4575.

[11] C. Papachristos, F. Mascarich, S. Khattak, T. Dang, and K. Alexis, "Localization uncertainty-aware autonomous exploration and mapping with aerial robots using receding horizon path-planning," *Autonomous Robots*, vol. 43, no. 8, pp. 2131–2161, 2019.

[12] A. Bircher, K. Alexis, M. Burri, P. Oettershagen, S. Omari, T. Mantel, and R. Siegwart, "Structural inspection path planning via iterative viewpoint resampling with application to aerial robotics," in *2015 IEEE International Conference on Robotics and Automation (ICRA)*. IEEE, 2015, pp. 6423–6430.

[13] M. Burri, J. Nikolic, C. Hürzeler, G. Caprari, and R. Siegwart, "Aerial service robots for visual inspection of thermal power plant boiler systems," in *2012 2nd international conference on applied robotics for the power industry (CARPI)*. IEEE, 2012, pp. 70–75.

[14] G. Paul, S. Webb, D. Liu, and G. Dissanayake, "Autonomous robot manipulator-based exploration and mapping system for bridge maintenance," *Robotics and Autonomous Systems*, vol. 59, no. 7-8, pp. 543–554, 2011.

[15] P. Arora and C. Papachristos, "Mobile manipulation–based deployment of micro aerial robot scouts through constricted aperture-like ingress points," in *2021 IEEE/RSJ International Conference on Intelligent Robots and Systems (IROS)*. IEEE, 2021, pp. 6716–6723.

[16] T. Tomic, K. Schmid, P. Lutz, A. Domel, M. Kassecker, E. Mair, I. L. Grixa, F. Ruess, M. Suppa, and D. Burschka, "Toward a fully autonomous uav: Research platform for indoor and outdoor urban search and rescue," *IEEE robotics & automation magazine*, vol. 19, no. 3, pp. 46–56, 2012.

[17] N. Michael, S. Shen, K. Mohta, V. Kumar, K. Nagatani, Y. Okada, S. Kiribayashi, K. Otake, K. Yoshida, K. Ohno *et al.*, "Collaborative mapping of an earthquake damaged building via ground and aerial robots," in *Field and service robotics*. Springer, 2014, pp. 33–47.

[18] S. Khattak, F. Mascarich, T. Dang, C. Papachristos, and K. Alexis, "Robust thermal-inertial localization for aerial robots: A case for direct methods," in *2019 International Conference on Unmanned Aircraft Systems (ICUAS)*. IEEE, 2019, pp. 1061–1068.

[19] J. Balaram, M. Aung, and M. P. Golombek, "The ingenuity helicopter on the perseverance rover," *Space Science Reviews*, vol. 217, no. 4, pp. 1–11, 2021.

[20] "irobot brings smart-mapping features to midrange i3, i3+ roombas." [Online]. Available: https://www.pcmag.com/news/irobot-brings-smart-mapping-features-to-midrange-i3-i3-plus-roombas

[21] "About the spot dock self-charging station." [Online]. Available: https://support.bostondynamics.com/s/article/About-the-Spot-Dock-self-charging-station

[22] "Boston dynamics' spot adds self-charging to live at remote sites forever." [Online]. Available: https://www.theverge.com/2021/2/2/22261932/boston-dynamics-spot-enterprise-self-charging-scout-web-based-control-software-robotic-arm

[23] "Dji dock,for roads less traveled." [Online]. Available: https://www.dji.com/dock

[24] "Skydio dock™ continuous inspection and mapping." [Online]. Available: https://www.skydio.com/skydio-dock

[25] "American robotics — fully-automated drones." [Online]. Available: https://www.american-robotics.com/

[26] Y. Mulgaonkar and V. Kumar, "Autonomous charging to enable long-endurance missions for small aerial robots," in *Micro-and Nanotechnology Sensors, Systems, and Applications VI*, vol. 9083. SPIE, 2014, pp. 404–418.

[27] F. Cocchioni, A. Mancini, and S. Longhi, "Autonomous navigation, landing and recharge of a quadrotor using artificial vision," in *2014 international conference on unmanned aircraft systems (ICUAS)*. IEEE, 2014, pp. 418–429.

[28] "Drone in a box icaros aerial intelligence," accessed: 2022-09-13. [Online]. Available: https://icarosgeospatial.com/drone-in-a-box-systems-fully-autonomous-drone-based-surveillance-inspections-systems/

[29] V. Fetisov and S. Akhmerov, "Charging stations with open contact pads for maintenance of aerial robots," in *2019 International Conference on Electrotechnical Complexes and Systems (ICOECS)*, 2019, pp. 1–6.

[30] D. Malyuta, C. Brommer, D. Hentzen, T. Stastny, R. Siegwart, and R. Brockers, "Long-duration fully autonomous operation of rotorcraft unmanned aerial systems for remote-sensing data acquisition," *Journal of Field Robotics*, vol. 37, no. 1, pp. 137–157, 2020.

[31] A. Rohan, M. Rabah, F. Asghar, M. Talha, and S.-H. Kim, "Advanced drone battery charging system," *Journal of Electrical Engineering & Technology*, vol. 14, no. 3, pp. 1395–1405, 2019.

[32] E. I. Shirokova, A. A. Azarov, N. G. Wilson, and I. B. Shirokov, "Precision positioning of unmanned aerial vehicle at automatic landing," in *2019 IEEE Conference of Russian Young Researchers in Electrical and Electronic Engineering (EIConRus)*. IEEE, 2019, pp. 1065–1069.

[33] P. R. Palafox, M. Garzón, J. Valente, J. J. Roldán, and A. Barrientos, "Robust visual-aided autonomous takeoff, tracking, and landing of a small uav on a moving landing platform for life-long operation," *Applied Sciences*, vol. 9, no. 13, p. 2661, 2019.

[34] E. Barrett, M. Reiling, S. Mirhassani, R. Meijering, J. Jager, N. Mimmo, F. Callegati, L. Marconi, R. Carloni, and S. Stramigioli, "Autonomous battery exchange of uavs with a mobile ground base," in *2018 IEEE International Conference on Robotics and Automation (ICRA)*. IEEE, 2018, pp. 699–705.

[35] A. Noth, "Design of solar powered airplanes for continous flight," Ph.D. dissertation, ETH Zurich, 2008.

[36] S. Morton, R. D'Sa, and N. Papanikolopoulos, "Solar powered uav: Design and experiments," in *2015 IEEE/RSJ international conference on intelligent robots and systems (IROS)*. IEEE, 2015, pp. 2460–2466.

[37] T. Henderson, D. Jenson, R. D'Sa, J. Kilian, and N. Papanikolopoulos, "Design and fabrication of a nomadic solar-powered quad-rotor," in *2020 International Conference on Unmanned Aircraft Systems (ICUAS)*. IEEE, 2020, pp. 1628–1635.

[38] R. D'Sa, T. Henderson, D. Jenson, M. Calvert, T. Heller, B. Schulz, J. Kilian, and N. Papanikolopoulos, "Design and experiments for a

transformable solar-uav," in *2017 IEEE International Conference on Robotics and Automation (ICRA)*. IEEE, 2017, pp. 3917–3923.

[39] T. Campi, F. Dionisi, S. Cruciani, V. De Santis, M. Feliziani, and F. Maradei, "Magnetic field levels in drones equipped with wireless power transfer technology," in *2016 Asia-Pacific International Symposium on Electromagnetic Compatibility (APEMC)*, vol. 1. IEEE, 2016, pp. 544–547.

[40] A. Bin Junaid, A. Konoiko, Y. Zweiri, M. N. Sahinkaya, and L. Seneviratne, "Autonomous wireless self-charging for multi-rotor unmanned aerial vehicles," *Energies*, vol. 10, no. 6, p. 803, 2017.

[41] S. A. Hoseini, J. Hassan, A. Bokani, and S. S. Kanhere, "In situ mimo-wpt recharging of uavs using intelligent flying energy sources," *Drones*, vol. 5, no. 3, p. 89, 2021.

[42] L. Blain, "In-flight charging gives drones unlimited autonomous range," *newatlas. com*, 2018.

[43] A. Noth, M. W. Engel, and R. Siegwart, "Flying solo and solar to mars," *IEEE robotics & automation magazine*, vol. 13, no. 3, pp. 44–52, 2006.

[44] A. Noth, W. Engel, and R. Siegwart, "Design of an ultra-lightweight autonomous solar airplane for continuous flight," in *Field and Service Robotics*. Springer, 2006, pp. 441–452.

[45] "Airbus zephyr," accessed: 2022-09-13. [Online]. Available: https://www.airbus.com/en/products-services/defence/uas/uas-solutions/zephyr

[46] R.-A. Peloquin, D. Thibault, and A. L. Desbiens, "Design of a passive vertical takeoff and landing aquatic uav," *IEEE Robotics and Automation Letters*, vol. 2, no. 2, pp. 381–388, 2016.

[47] É. Tétreault, D. Rancourt, and A. L. Desbiens, "Active vertical takeoff of an aquatic uav," *IEEE Robotics and Automation Letters*, vol. 5, no. 3, pp. 4844–4851, 2020.

[48] P. Arora, S. J. Carlson, T. Karakurt, and C. Papachristos, "Deep-learned autonomous landing site discovery for a tiltrotor micro aerial vehicle," in *2022 International Conference on Unmanned Aircraft Systems (ICUAS)*. IEEE, 2022, pp. 255–262.

[49] Z. Ge, S. Liu, F. Wang, Z. Li, and J. Sun, "Yolox: Exceeding yolo series in 2021," *arXiv preprint arXiv:2107.08430*, 2021.

[50] S. J. Carlson and C. Papachristos, "Solar energy harvesting for a land-to-recharge tiltrotor micro aerial vehicle," in *2022 IEEE Aerospace Conference (AEROCONF)*, 2022, pp. 1–8.

[51] P. De Petris, S. Khattak, M. Dharmadhikari, G. Waibel, H. Nguyen, M. Montenegro, N. Khedekar, K. Alexis, and M. Hutter, "Marsupial walking-and-flying robotic deployment for collaborative exploration of unknown environments," *arXiv preprint arXiv:2205.05477*, 2022.